Chapter 7

Finite Element Analysis of Bias Extension Test of Dry Woven

Samia Dridi

Additional information is available at the end of the chapter

http://dx.doi.org/10.5772/46161

1. Introduction

In the composite industry, the shearing behaviour of dry woven plays a crucial role in fabric formability when doubly curved surfaces must be covered [1-9]. The ability of fabric to shear within a plain enables it to fit three-dimensional surfaces without folds [10-12].

It has been proved that shear rigidity can be calculated from the tensile properties along a 45° bias direction. Bias Extension tests are simple to perform and provide reasonably repeatable results [13-14]. Extensive investigations have been carried out on the textile fabric in Bias Extension test [15]

The tests were conducted simply using two pairs of plates, clamping a rectangular piece of woven material such that the two groups of yarns are orientated ±45° to the direction of external tensile force. The ratio between the initial length and width of the specimen is defined as aspect ratio:

$\lambda = l_0/w_0$ (see Figure 1a).

In the case of λ =2, the deformed configuration of the material can be represented by Figure1b, which includes seven regions. Triangular regions C adjacent to the fixture remain undeformed, while the central square region A and other four triangular regions B undergo shear deformation [16-17].

The present chapter focuses on numerical analysis of Bias Extension test using an orthotropic hyperelastic continuum model of woven fabric.

In the first, analytical responses of the Bias Extension test and the traction test on 45° are developed using the proposed model. Strain and stress states in specimen during these tests are detailed.

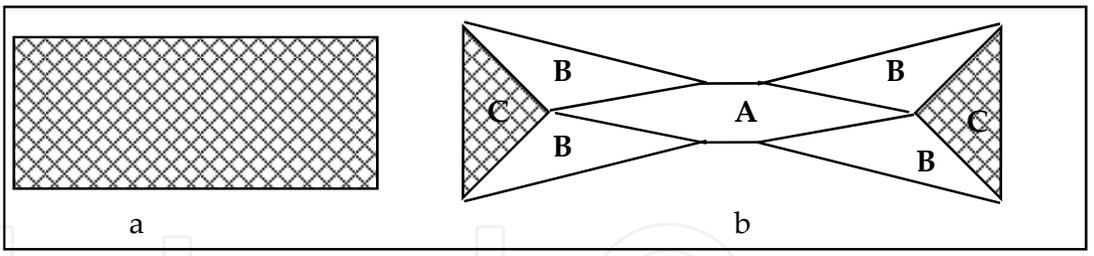

Figure 1. Kinematic of Bias Extension test, a: Initial state, b: Deformed state

In the second, the proposed model is implanted into Abaqus/Explicit to simulate the Bias Extension test of three aspect ratios.

Exploiting numerical results, we studied the effect of the ratio between shearing and traction rigidities on homogeneities of stress and strain in the central zone of three Finite Element Models (FEM).

2. The proposed hyperelastic model

One of significant characteristics of the woven structure is the existence of two privileged material directions: warp and weft. We considered that the fabric is a continuous structure having two privileged material directions defined by the two unit tensors $\boldsymbol{M_1}$ and $\boldsymbol{M_2}$ as follows:

$$\boldsymbol{M_1} = \vec{M}_1 \otimes \vec{M}_1 \; ; \; \boldsymbol{M_2} = \vec{M}_2 \otimes \vec{M}_2 \tag{1}$$

Where $\vec{M}_1$ and $\vec{M}_2$ are two unit vectors carried by two yarns directions. The sign $\otimes$ indicate the tensor product. In the reference configuration, these privileged material directions are supposed to be orthogonal and they are defined by $\boldsymbol{g_1}$ and $\boldsymbol{g_2}$ presented by Equation 2.

$$\boldsymbol{g_1} = \vec{g}_1 \otimes \vec{g}_1 \; , \; \boldsymbol{g_2} = \vec{g}_2 \otimes \vec{g}_2 \tag{2}$$

In Lagrangian formulation, the hyperelastic behavior is defined by the strain energy function $W(\boldsymbol{E})$ depending of Green-Lagrange tensor components [18-21].

The second Piola Kirchhoff stress tensor $\boldsymbol{S}$ derives is presented in Equation 3:

$$\boldsymbol{S} = \frac{\partial W}{\partial \boldsymbol{E}} \tag{3}$$

The physical behaviour is completely defined by the choice of $W(\boldsymbol{E})$. The woven structures is very thin, we are interested more particularly in plane solicitations (plane stress or strain) in the plan ($\vec{g}_1$, $\vec{g}_2$). We supposed that $W(\boldsymbol{E})$ is an isotropic function of variables ($\boldsymbol{E}$, $\mathbf{g_1}$, $\mathbf{g_2}$). Using the representation theorems of isotropic functions, strain energy function $W(\boldsymbol{E})$ depends of invariants:

$$\boldsymbol{g_i}:\boldsymbol{E} \; , \; \boldsymbol{g_i}:\boldsymbol{E}^2 \; , \; tr(\boldsymbol{E}^3) \;\; (i = 1..2) \tag{4}$$

We choose following invariants to present the strain energy function:

$$W(\boldsymbol{E}) = W(I_1, I_2, I_{12}) \tag{5}$$

Where

$$I_i = \boldsymbol{g_i}:\boldsymbol{E} \ \left(i = 1..2\right) \ ; \ I_{12} = \frac{1}{2}(\boldsymbol{g_1 E}:\boldsymbol{E g_2})^{1/2} \tag{6}$$

I_i measured elongations along directions $\vec{g}_i$. I_{12} measured the sliding in the plane ($\vec{g}_1$, $\vec{g}_2$) witch is the angle variation between warp and weft direction. Components $E_{g_{ij}}$ of $\boldsymbol{E}$ in the reference system ($\vec{g}_1$, $\vec{g}_2$), are defined as follows:

$$I_i = E_{gij} = \frac{1}{2}(\delta_1^2 - 1) \ , i = 1..2, I_{12} = \left|E_{g12}\right| = \frac{1}{2}\delta_1\delta_2\left|\cos(\theta)\right| \tag{7}$$

δ_1 and δ_2 are yarns extensions (ratio between deformed and initial lengths) along directions of $\vec{g}_1$ and $\vec{g}_2$. θ is the angle between $\vec{M}_1$ and $\vec{M}_2$.

The second Piola Kirchhoff stress tensor $\boldsymbol{S}$ can be written as:

$$\boldsymbol{S}=\frac{\partial W}{\partial I_1}\boldsymbol{g_1} + \frac{\partial W}{\partial I_2}\boldsymbol{g_2} + \frac{\partial W}{\partial I_{12}}\frac{1}{2I_{12}}(\boldsymbol{g_1 E g_2} + \boldsymbol{g_2 E g_1}) \tag{8}$$

A simplified hyperplastic model is proposed. It is based on following assumptions:

- The coupling between I_{12} and I_i is neglect,
- The strain energy function $W(\boldsymbol{E})$ is expressed by Equation 9:

$$W = \frac{1}{2}k_1 I_1^2 + \frac{1}{2}k_2 I_2^2 + k_{12} I_1 I_2 + k_3 I_{12}^2 \tag{9}$$

This leads to the constitutive equation:

$$\boldsymbol{S} = (k_1 I_1 + k_{12} I_2)\boldsymbol{g_1} + (k_2 I_2 + k_{12} I_1)\boldsymbol{g_2} + k_3(\boldsymbol{g_1 E g_2} + \boldsymbol{g_2 E g_1}) \tag{10}$$

So k_1 and k_2 presented tensile rigidities in yarns directions. k_{12} described the interaction between two groups of yarns. k_3 presented the shearing rigidity of woven.

The relation between components S_{gij} of second Piola Kirchhoff stress tensor $\boldsymbol{S}$ and E_{gij} of Green Lagrange strain tensor $\boldsymbol{E}$ in the base $\vec{g}_i$ can be presented by one of flowing expressions

$$\begin{bmatrix} S_{g11} \\ S_{g22} \\ S_{g12} \end{bmatrix} = \begin{bmatrix} k_1 & k_{12} & 0 \\ k_{12} & k_2 & 0 \\ 0 & 0 & k_3 \end{bmatrix} \begin{bmatrix} E_{g11} \\ E_{g22} \\ E_{g12} \end{bmatrix} \tag{11}$$

$$\begin{bmatrix} E_{g11} \\ E_{g22} \\ E_{g12} \end{bmatrix} = \begin{bmatrix} c_1 & c_{12} & 0 \\ c_{12} & c_2 & 0 \\ 0 & 0 & c_3 \end{bmatrix} \begin{bmatrix} S_{g11} \\ S_{g22} \\ S_{g12} \end{bmatrix} \tag{12}$$

Where:

$$c_1 = \frac{k_2}{k_1 k_2 - k_{12}^2}, c_2 = \frac{k_1}{k_1 k_2 - k_{12}^2}, c_3 = \frac{1}{k_3}, c_{12} = \frac{-k_{12}}{k_1 k_2 - k_{12}^2} \tag{13}$$

2.1. Out-axes tensile test: Tensile test on 45°

In tis parts the proposed hyperelastic model is used to study the mechanical behaviour during the out-axes tensile test of the dry woven.

Out-axes tensile test is a tensile test exerted on a fabric but according to a direction which is not necessarily warp or weft directions [22]. In the case of anisotropic behavior stress and strains tensors have not, in general, the same principal directions. During this test, the simple is subjected to a shearing. Particular precautions must be taken to ensure a relative homogeneity of the test [23].

We considered a tensile test along a direction $\vec{E}_1$ forming an angle ψ_0 with orthotropic direction $\vec{g}_i$ (Figure.2).

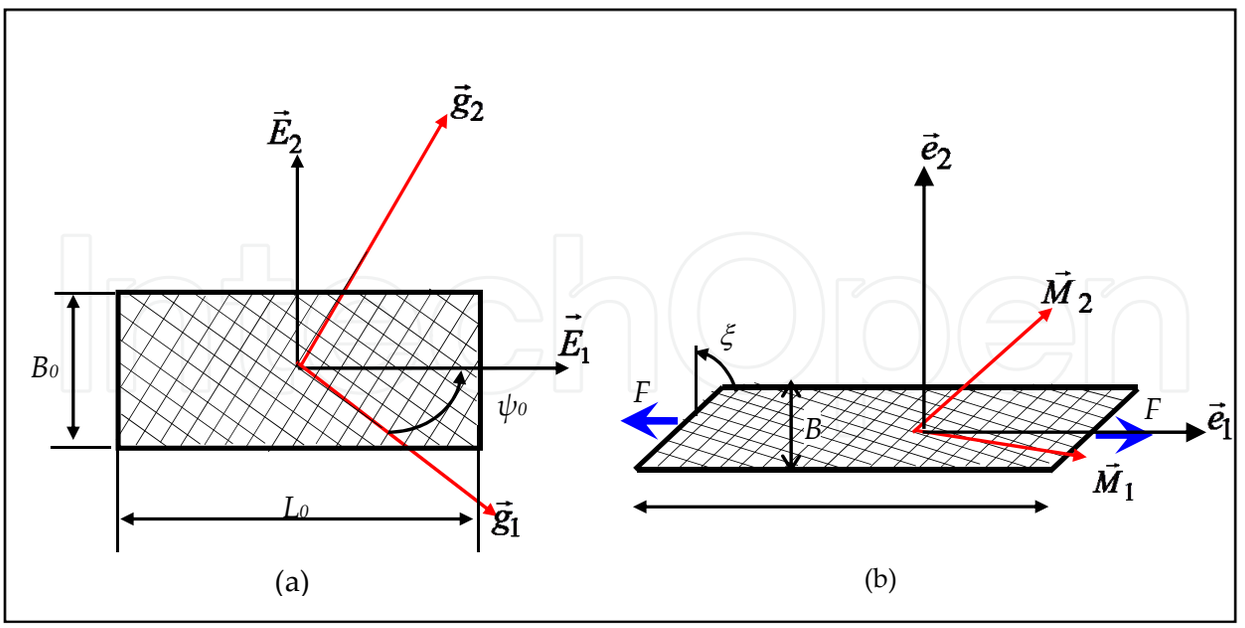

Figure 2. Kinematics of Out-axes tensile test, a: Reference configuration, b: Deformed configuration.

In the base $\vec{e}_i$, components of the second Piola Kirchhoff tensor ***S*** and the Gradient of transformation tensor ***F*** are as follows [23]

$$\boldsymbol{S}_{/\vec{e}_i} = \begin{bmatrix} S & 0 \\ 0 & 0 \end{bmatrix}, \boldsymbol{F}_{/\vec{e}_i} = \begin{bmatrix} f_1 & f_1\gamma \\ 0 & f_2 \end{bmatrix} \tag{14}$$

Where:

$$f_1 = \frac{L}{L_0}; f_2 = \frac{B}{B_0}; \gamma = \frac{f_2}{f_1} tg(\xi) \tag{15}$$

Let $P = \frac{F}{S_0}$ where F is the tensile force and S_o is the initial cross section of the specimen. P is related to S by:

$$P = \frac{F}{S_0} = f_1 S \tag{16}$$

The components of the Green–Lagrange strain tensor ***E,*** in the base $\vec{e}_i$, are as follows:

$$\boldsymbol{E}_{/\vec{e}_i} = \begin{bmatrix} E_{11} & E_{12} \\ E_{12} & E_{22} \end{bmatrix} \tag{17}$$

Where

$$2E_{11} = f_1^2 - 1;\ 2E_{22} = f_2^2 - 1 + f_1^2\gamma^2;\ 2E_{12} = f_1^2\gamma \tag{18}$$

The response of the model presented by Equation 8 for this solicitation can be summarised as follows:

$$P = \frac{f_1 E_{11}}{C(\psi_0)};\ E_{22} = -\nu(\psi_0)E_{11};\ E_{12} = g(\psi_0)E_{11} \tag{19}$$

Where:

$$\begin{aligned} C(\psi_0) &= c_1\cos^4(\psi_0) + c_2\sin^4(\psi_0) + \frac{1}{2}(c_3 + c_{12})\sin^2(2\psi_0) \\ \nu(\psi_0 &= \frac{\left[(2c_3 + 2c_{12} - c_1 - c_2)\sin^2(2\psi_0) - c_{12}\right]}{4C(\psi_0)} \\ g(\psi_0) &= \frac{\sin(2\psi_0)\left[c_1\cos^2(\psi_0) - c_2\sin^2(\psi_0) - (c_3 + c_{12})\cos(2\psi_0)\right]}{2C(\psi_0)} \end{aligned} \tag{20}$$

The tensile test on 45° is a particular case of out-axes tensile tests where ψ_0=45). To replacing ψ_0 by 45°, Equation 20 became like the following:

$$C_{45} = \frac{1}{2k_3} + \frac{k_1 + k_2 + 2k_{12}}{4(k_1k_2 - k_{12}^2)},\ \nu_{45} = \frac{\left[(2c_3 + 2c_{12} - c_1 - c_2) - c_{12}\right]}{4C_{45}},\ g_{45} = -\frac{c_2}{2C_{45}} \tag{21}$$

S_1 and S_2 are respectively the maximum and the minimum Eigen values of Piola Kirchhoff tensor $\boldsymbol{S}$ .In Tensile test on 45°, Equation 14 shows that:

$$\frac{S_2}{S_1} = 0 \tag{22}$$

The expression of the applied force F is deducted from Equation 16:

$$F = PS_0 = \frac{2k_3 S_0 f_1 (f_1^2 - 1)(k_1 k_2 - k_{12}^2)}{2k_1 k_2 - 2k_{12}^2 + k_3 (k_1 + k_2 - 2k_{12})} \tag{23}$$

For a balanced woven (k_1=k_2=k) where the interaction between yarns is neglected (k_{12}=0), the expression of F became:

$$F = \frac{k_3 k S_0 f_1 (f_1^2 - 1)}{k + k_3} \tag{24}$$

The ratio between the minimum and the maximum Eigen values of Green Lagrange tensor ***E.***, in the tensile test with 45°, is given by Equation 25:

$$\frac{E_2}{E_1} = -\frac{k - k_3}{k_3 + k} \tag{25}$$

2.2. Bias extension test

To explainer the pure shearing test of woven fabric, it has been noted that woven cloths in general deform as a pin-jointed-net (PJN) [24-28]. Yarns are considered to be inextensible and fixed at each cross-over point, rotating about these points like it is shown in Figure 3.

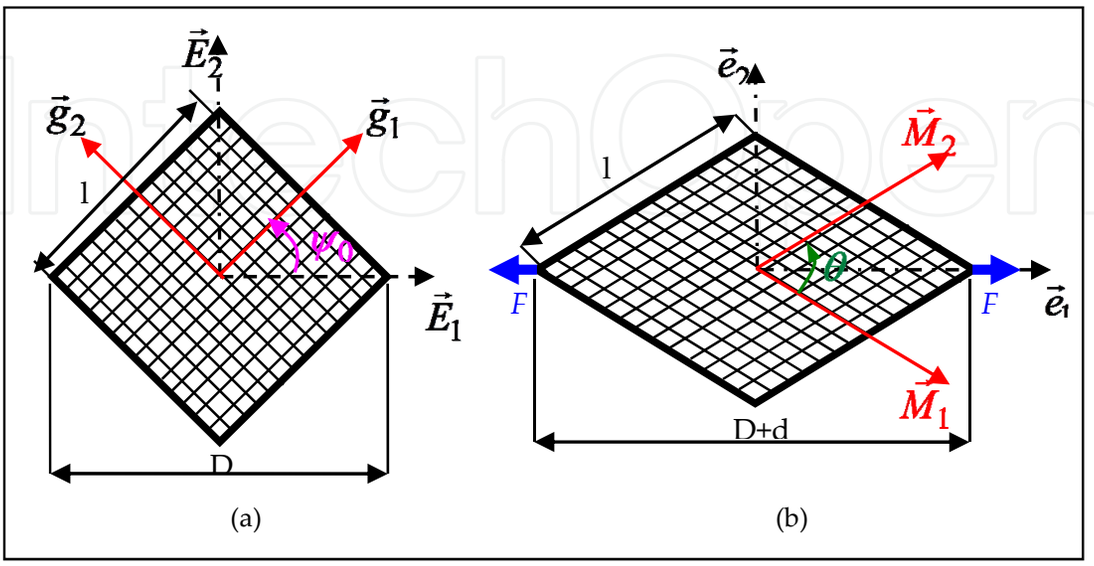

Figure 3. Kinematics Pure shear a: Reference configuration, b: Deformed configuration

During the Bias Extension test, the pure shearing occurred in the central zone A and the shear angle φ is defined by Equation 26:

$$\varphi = \frac{\pi}{2} - \theta = \frac{\pi}{2} - 2a\cos(\frac{D+d}{\sqrt{2}D}) \tag{26}$$

The Gradient of Transformation tensor $\boldsymbol{F}$ is presented by Equation 27:

$$\boldsymbol{F}_{/Ei,ei} = \begin{bmatrix} f_1 & 0 \\ 0 & f_2 \end{bmatrix} = \begin{bmatrix} \cos(\frac{\varphi}{2}) + \sin(\frac{\varphi}{2}) & 0 \\ 0 & \cos(\frac{\varphi}{2}) - \sin(\frac{\varphi}{2}) \end{bmatrix} \tag{27}$$

Using the proposed model, components S_{ij} ,E_{ij} of the second Piola Kirchhoff stress and Green Lagrange strain tensors are given, in the base $\vec{e}_i$, as follows:

$$\boldsymbol{S}_{/\vec{e}_i} = S(\varphi)\begin{bmatrix} 1 & 0 \\ 0 & -1 \end{bmatrix} \text{ where } S(\varphi) = \frac{1}{2}k_3\sin(\varphi) \tag{28}$$

$$\boldsymbol{E}_{/e_i} = E(\varphi)\begin{bmatrix} 1 & 0 \\ 0 & -1 \end{bmatrix} \text{ where } E(\varphi) = \frac{1}{2}\sin(\varphi) \tag{29}$$

Thus

$$\frac{S_2}{S_1} = -1 \tag{30}$$

And

$$\frac{E_2}{E_1} = -1 \tag{31}$$

Where S_1 and S_2 are respectively the maximum and the minimum Eigen values of the second Piola Kirchhoff tensor $\boldsymbol{S}$ and E_1 and E_2 are respectively the maximum and the minimum Eigen values of Green Lagrange tensor $\boldsymbol{E}$.

The internal power per unit of volume in zone A is defined by Equation 32:

$$\omega a = \boldsymbol{S}_A : \dot{\boldsymbol{E}}_A = 2S(\varphi)\dot{E}(\varphi) = \frac{1}{4}k_3\sin(2\varphi)\dot{\varphi} \tag{32}$$

To calculate to internal power per unit of volume in zone B we replace φ by $\frac{\varphi}{2}$ in Equation 32:

$$\omega b = \boldsymbol{S}_{\boldsymbol{B}} : \dot{\boldsymbol{E}}_{\boldsymbol{B}} = 2S(\frac{\varphi}{2})\dot{E}(\frac{\varphi}{2}) = \frac{1}{8}k_3\sin(\varphi)\dot{\varphi} \tag{33}$$

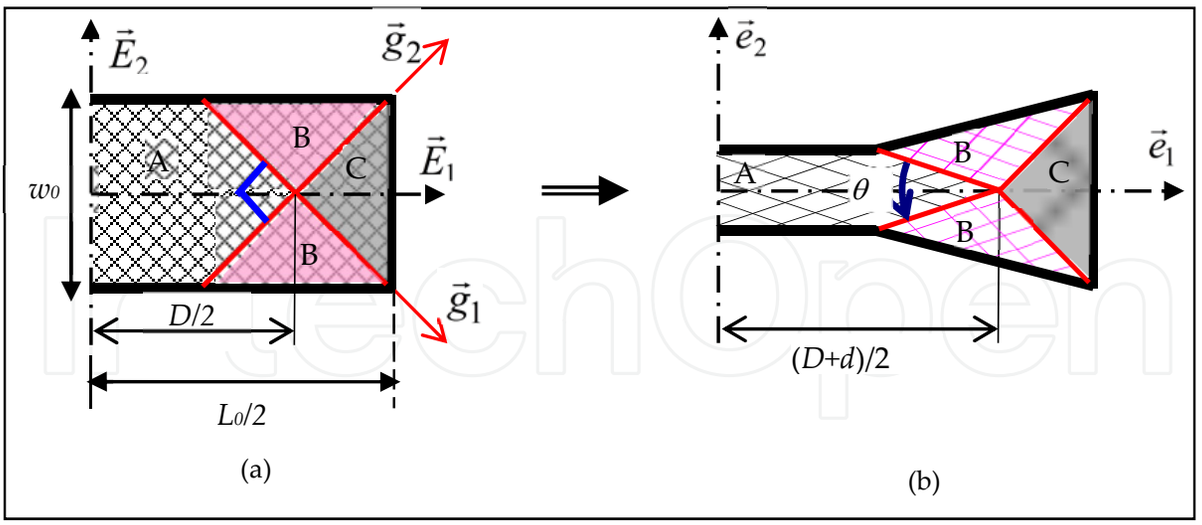

Figure 4. Kinematic of Bias Extension Test, a: initial configuration, b: deformed configuration

The total internal power in the specimen is given by Equation 34:

$$P\,\text{int} = Va.\omega a + Vb.\omega b \tag{34}$$

Where Va and Vb are respectively the initial volume in zones A and B defined as follows

$$\begin{aligned} Vb &= e_0 w_0^2 \\ Va &= e_0(Dw_0 - \frac{w_0^2}{2}) = e_0 Dw_0 - \frac{1}{2}Vb \end{aligned} \tag{35}$$

The External power is defined as:

$$Pext = F.\dot{d} = \frac{1}{2}FDf_2\dot{\varphi} \tag{36}$$

The equality between internal and external powers allows to determinate the expression of applied force F given by Equation 37:

$$F = e_0 w_0 f_1 k_3 \sin(\varphi)[1 + \frac{1}{4(\lambda - 1)\cos(\varphi)}(1 - 2\cos(\varphi))] \tag{37}$$

Where $\lambda = \frac{L_0}{w_0}$ is the aspect ratio.

3. Numerical simulation of Bias Extension test

In this section, we simulated the Bias Extension test (BE) using the hyperelastic proposed model implanted into Abaqus/Explicit thought user material subroutine (VUMAT). Out put of the VUMAT are stress components of Cauchy tensor projected in the Green-Nagdi basis,

component of the second Piola Kirchhoff tensor ***S***, and the Green Lagrange tensor ***E*** projected in $(\vec{g}_1, \vec{g}_2)$. We can also drew curves of Fore versus displacement.

The fabric is modelling by rectangular part meshed by continuum element (M3D4R).The boundary condition of model is presented in Figure 5a.

[29-30] compared the numerical results for the biased mesh and the aligned mesh and they proved that by using the biased mesh (Figure 5b), where the fibres are run diagonally across the rectangular element, neither the deformation profile nor the reaction forces are predicted correctly, for this we used the aligned mesh (Figure 5c).

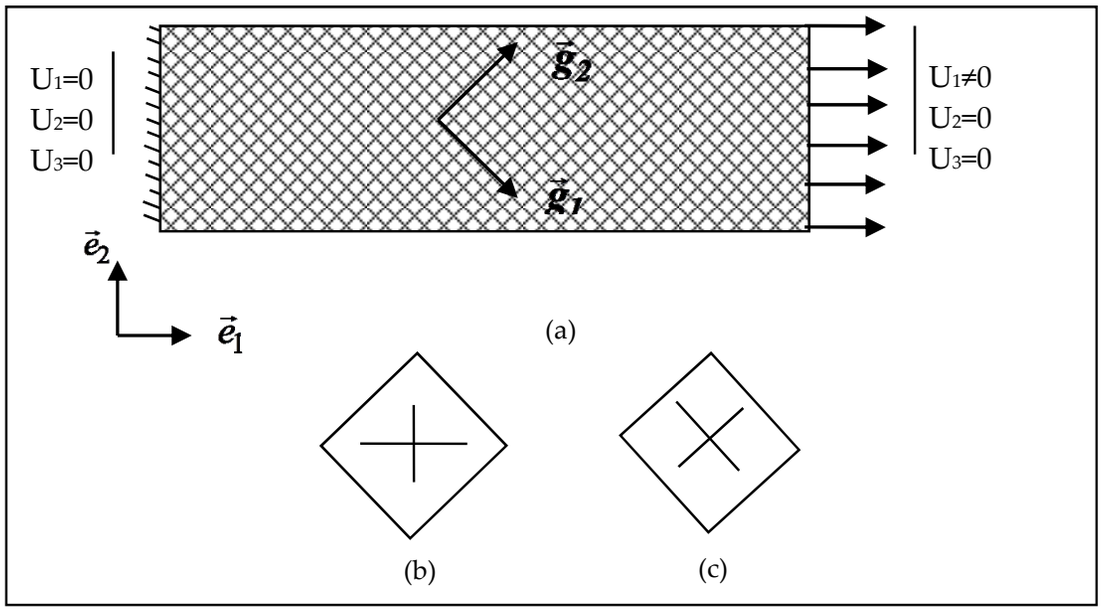

Figure 5. FEM mesh for the Bias Extension simulation, a: boundary condition of FEM, b: biased mesh, c: aligned mesh.

In order to simplify the problem, we used a balanced woven ($k_1=k_2=k$=700 N/mm²) and we ignored the interaction between extension in yarns direction (k_{12}=0). The analysis is done for three different FEM with the same thickness of 0.2mm. Dimensions of FEM are presented in table 1.

MEF	Length(mm)	Width(mm)	Aspect ratio: λ
1	100	50	2
2	150	50	3
3	200	50	4

Table 1. Dimensions of samples

This analysis is realised on four values of the ratio between shearing and tensile rigidities $(\frac{k_3}{k} = 0.007, 0.02, 0.1, 0.3, 1)$ along three paths in FEM (see Figure 6).

The first path is longitudinal line in the middle of FEM. It joined zones A and C, the second path is along the yarn direction and the third path is transversal middle line Flowing results are illustrated for a displacement of 10% of initial length.

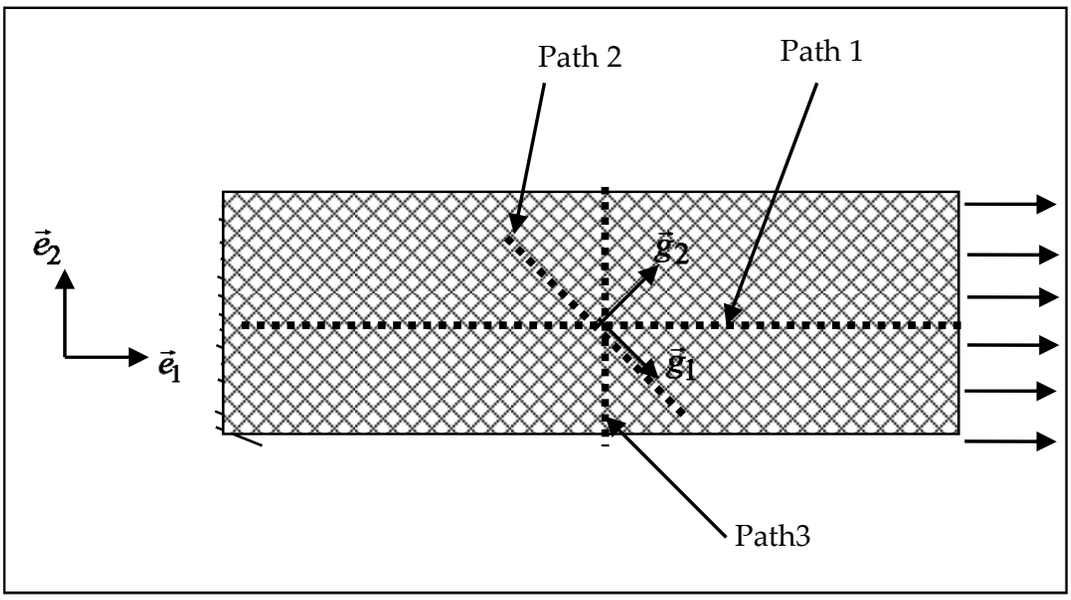

Figure 6. Different paths used in analysis

The deformed mesh with the contour of the Green Lagrange shear strain is shown in Figure7. We noticed that appearance of three discernible deformation zones of the Bias Extension test in three FEM. No significant deformation occurred in zone C. The main mode of deformation in zone A is the shearing. The most deformation of the fabric occurs in this zone.

In to order to study homogeneities of stress and strain states, we compared the analytical and the numerical results of strain and stress along three paths of Figure (6).

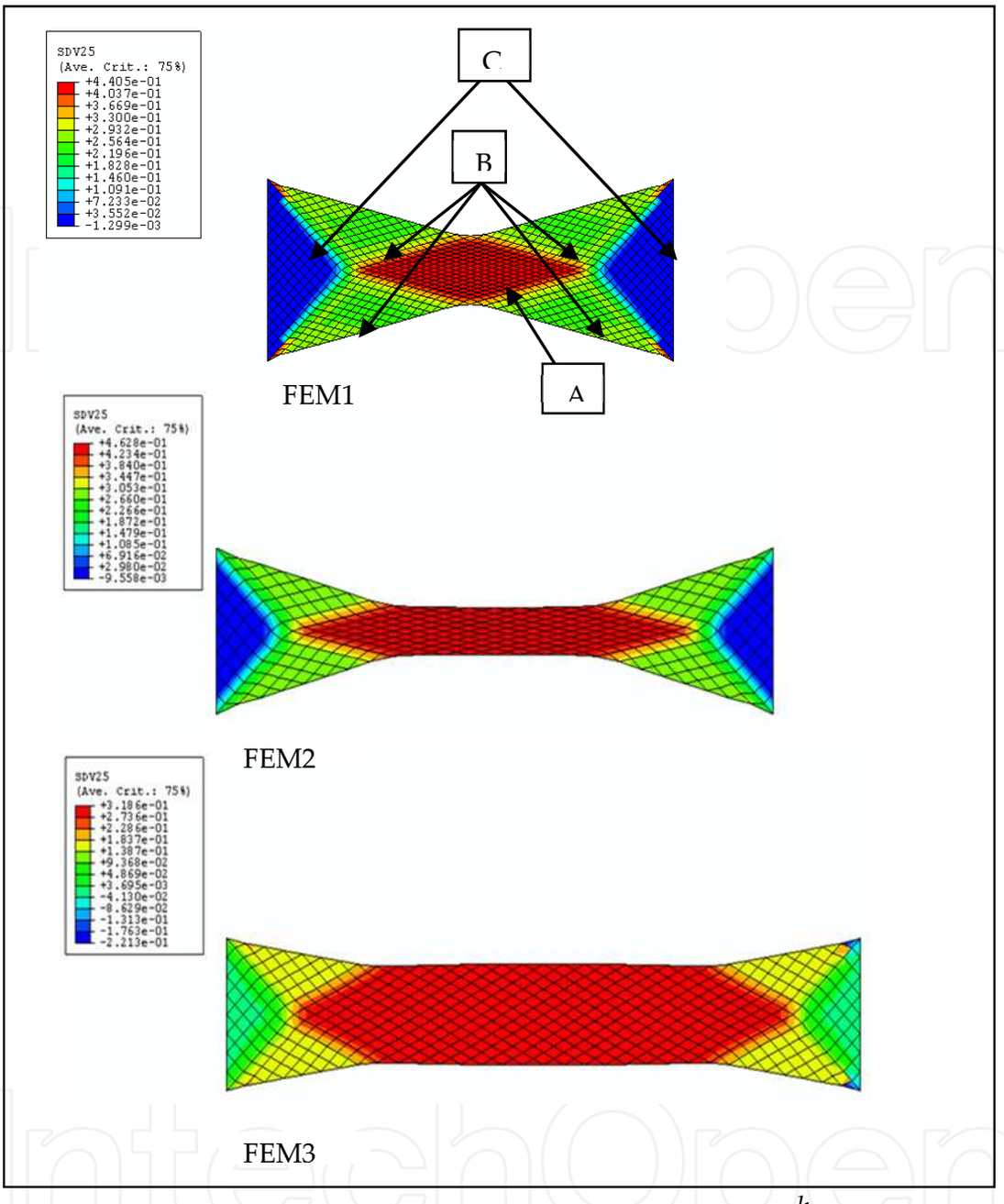

Figure 7. Deformed mesh with contour of Green Lagrange shear strain E_{12} for $\frac{k_3}{k}$ =0.007 and U_1=40mm.

3.1. Strain state

Figure 8 shows the variation of the maximum principal E_1 of Green Lagrange along the first path. We noticed that E_1 is symmetric with regard to the centre of the FEM. For the higher value of ratio of rigidities ($\frac{k_3}{k}$ =1), E_1 is homogenous and it conformed to the predicted value in the case of isotropic elastic material. To decreasing the ratio of rigidities ($\frac{k_3}{k}$), the central

zone characterised by the higher value of E_1. En addition, we observed the appearance of two zones where the strain is not more important. In the first hand, to comparing with the analytical value of E_1 in the central zone, the numerical values of E_1 is closely to that predicted in the Bias Extension test for the few shearing rigidity. Zones C coincided with ends of the path where the deformation was not more significant. In another hand, we remarked that in the central zone of the path, the deformation is not homogenous especially in FEM1and FEM2. For more analyse the strains state in FEM, Figure 9 presented the evolution of $\frac{E_2}{E_1}$, along the first path. It is clear that to decreasing $\frac{k_3}{k}$, the value of $\frac{E_2}{E_1}$ tends to (-1) in three FEM. This proved that, in spite of the low displacement, the deformation in Bias Extension test is influenced by the ratio between shearing and tensile rigidities of the woven.

3.2. Stress state

Comparing the numerical and the analytical values of $\frac{S_2}{S_1}$, we determinate the stress state in different FEM for an displacement of 10% along the first path .

Figure10 show that to decreasing $\frac{k_3}{k}$, the value of $\frac{S_2}{S_1}$ decrease but never achieved (-1).

Indeed, if this simulation is interpreted like a Bias Extension test, $\frac{S_2}{S_1}$ should be verifying Equation 30 in the central zone. However the ratio of principal strain is approximately equal to 0. So it is conforming to Equation 22, and the stress state is the traction state.

In addition to varying the value of $\frac{k_3}{k}$, we evaluated the ratio of strain versus the ratio of stress in the central element of FEM. In Figure12, it can be noticed that in FEM1, to reducing the value of $\frac{k_3}{k}$, $\frac{E_2}{E_1}$ tend to (-1) and it conformed to the predicted value by Equation 31 for a few values of $\frac{k_3}{k}$. But $\frac{S_2}{S_1}$ have a negative value and it remain different to (-1). In FEM2, it was visibly that $\frac{S_2}{S_1}$ stayed proximity null for different value of $\frac{k_3}{k}$ thus it verified Equation 22 but $\frac{E_2}{E_1}$ tend to (-1) for few values of $\frac{k_3}{k}$. In FEM3, it was clear that for few value of $\frac{k_3}{k}$, $\frac{E_2}{E_1}$ tend to (-1), but the $\frac{S_2}{S_1}$ had positive values. Consequently, the shearing deformation in Bias Extension test depends of the ratio of rigidities between shearing and tensile, but the stress state is always the tensile stress.

FEM1

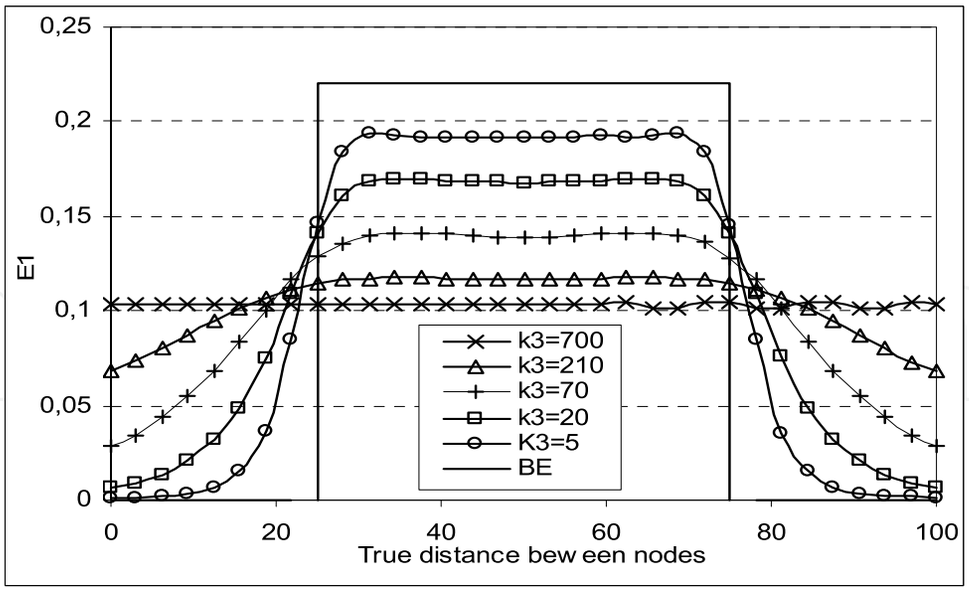

FEM2

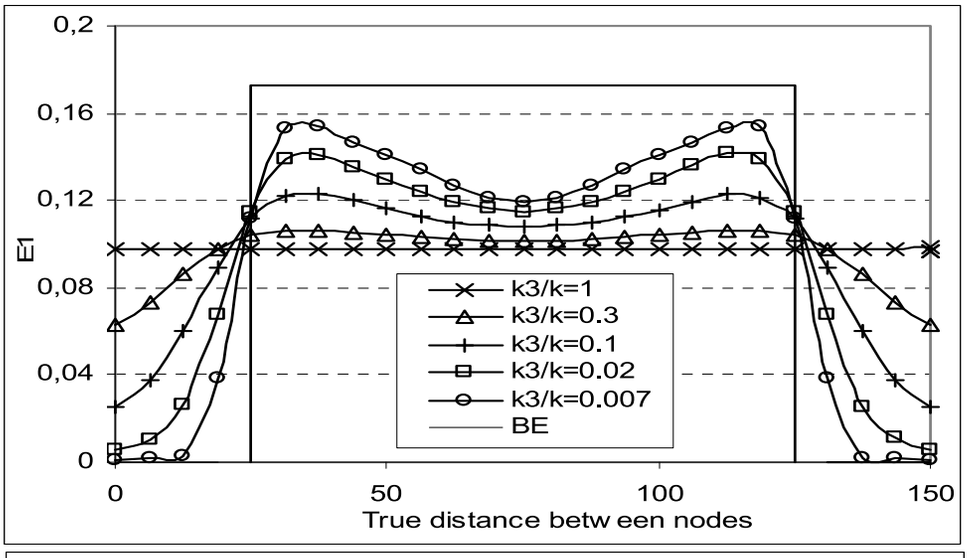

FEM3

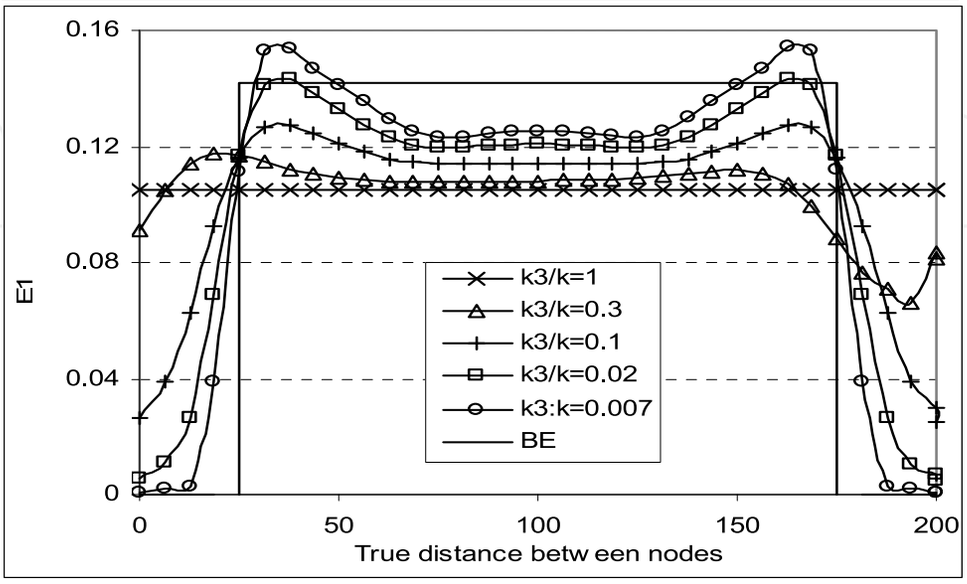

Figure 8. Variation of Maximum principal of Green Lagrange strain E_1 along the path1

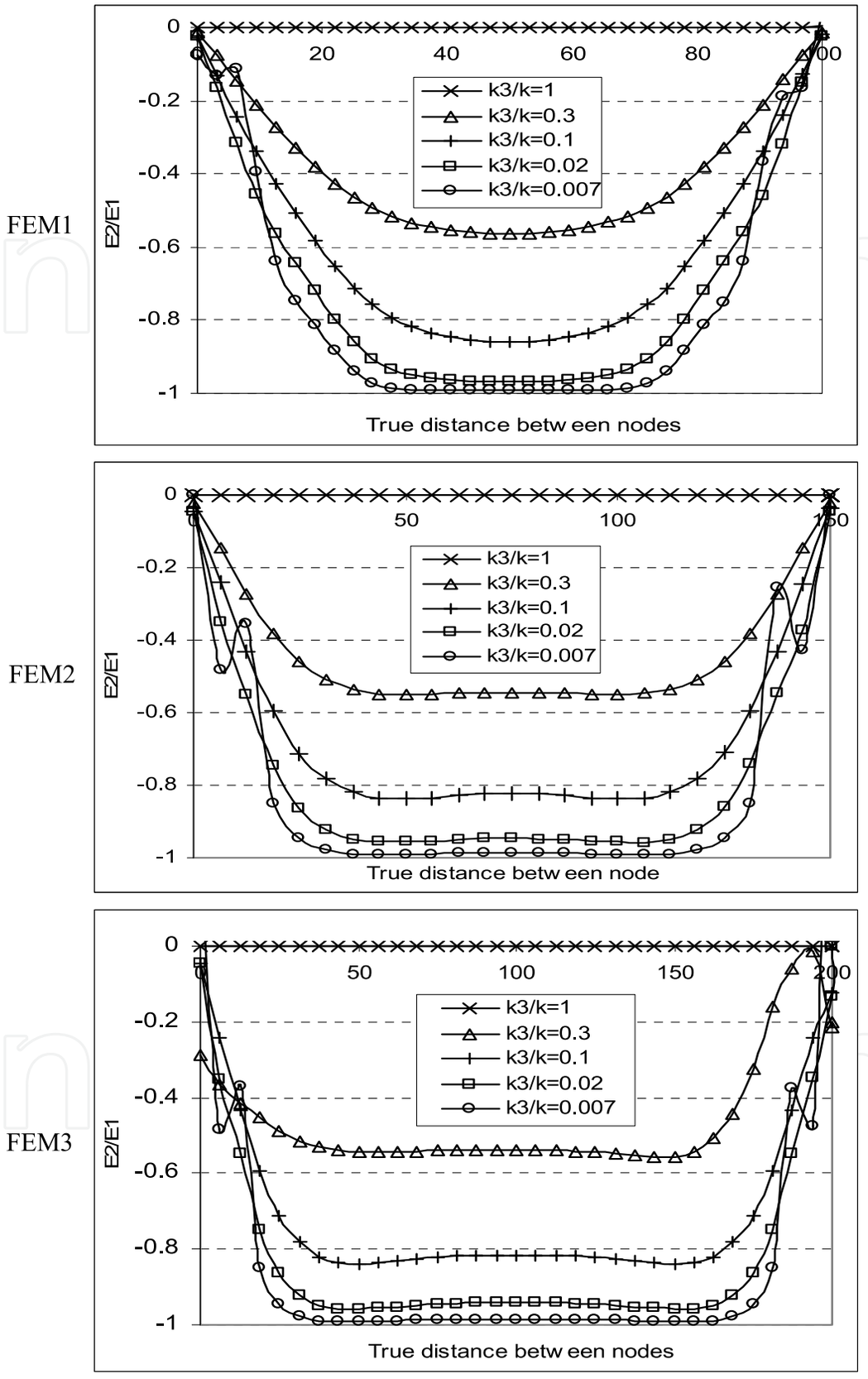

Figure 9. Variation of $\frac{E_2}{E_1}$ along the path 1

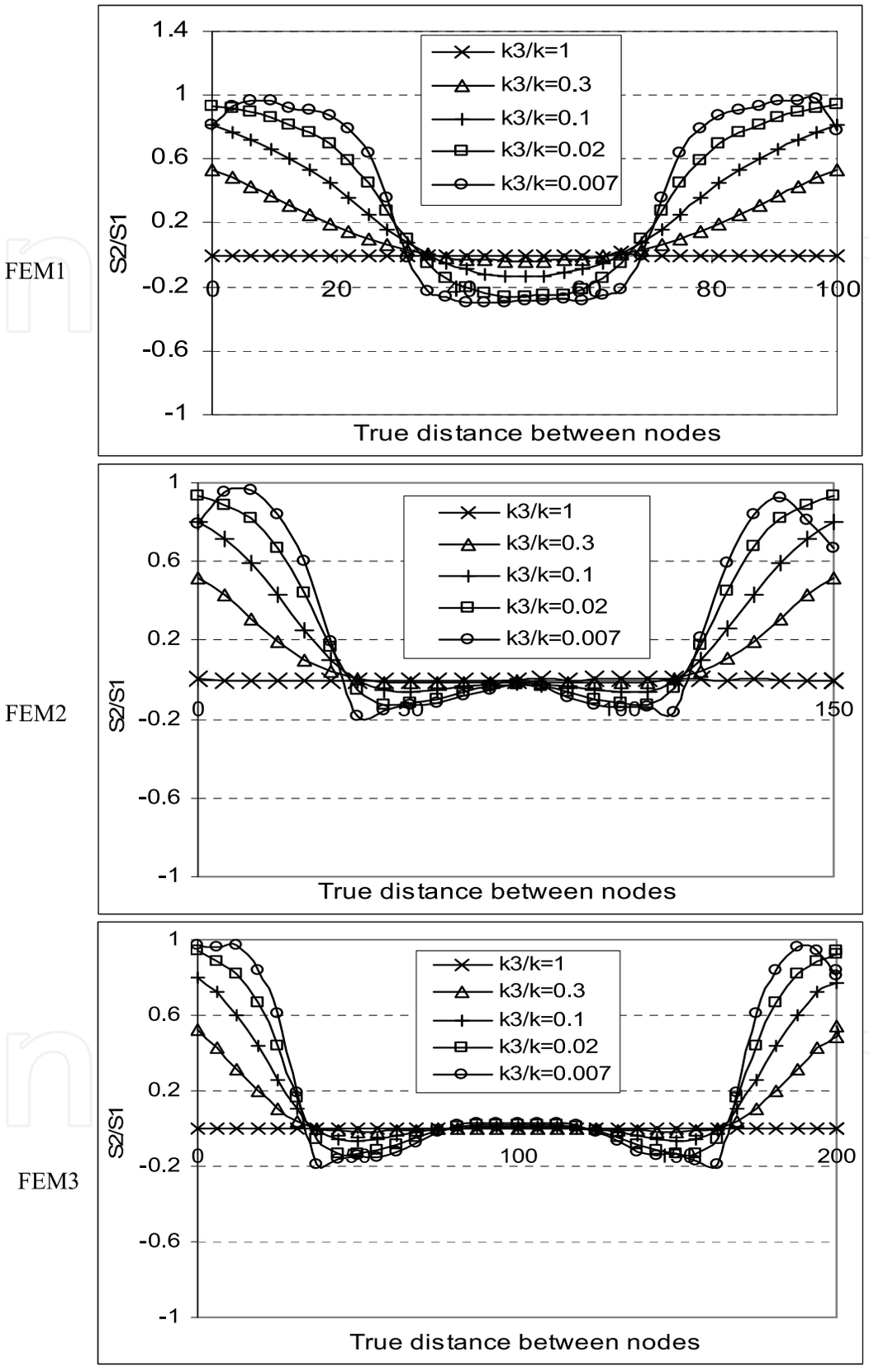

Figure 10. Variation of $\frac{S_2}{S_1}$ along path 1.

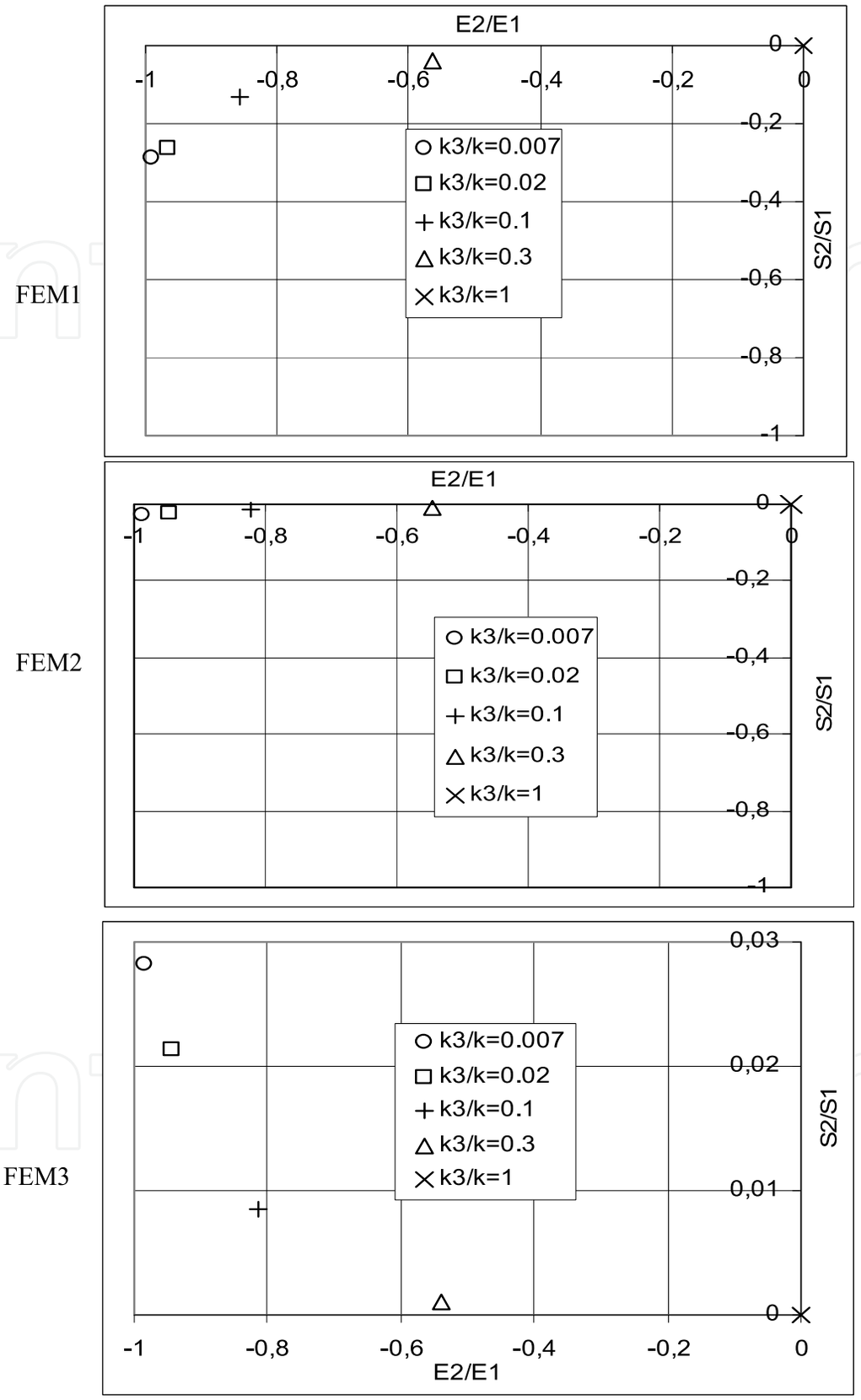

Figure 11. Variation of $\frac{S_2}{S_1}$ versus $\frac{E_2}{E_1}$ along path 1.

3.3. Angle between yarns

In this section, we compared between the numerical and the predicted values of the angle between yarns, along the first path.

Using the proposed model, the numerical angle between yarns is given by the following expression:

$$\theta_N = \arccos\left(\sqrt{\frac{(2E_{g12})^2}{(2E_{g22}+1)(2E_{g11}+1)}}\right) \tag{38}$$

In the case of the Bias Extension test, the predict angle between yarns in the central zone A is given by Equation 39:

$$\theta_B = 2\arccos\left(\frac{D+d}{\sqrt{2}D}\right) \tag{39}$$

The predict angle between yarns in the Tensile test in 45° is given by Equation 41:

$$\theta_T = \arccos\left(\frac{E_{11}(1-\nu_{45})}{\sqrt{(E_{11}+E_{22}+1)^2}}\right) \tag{40}$$

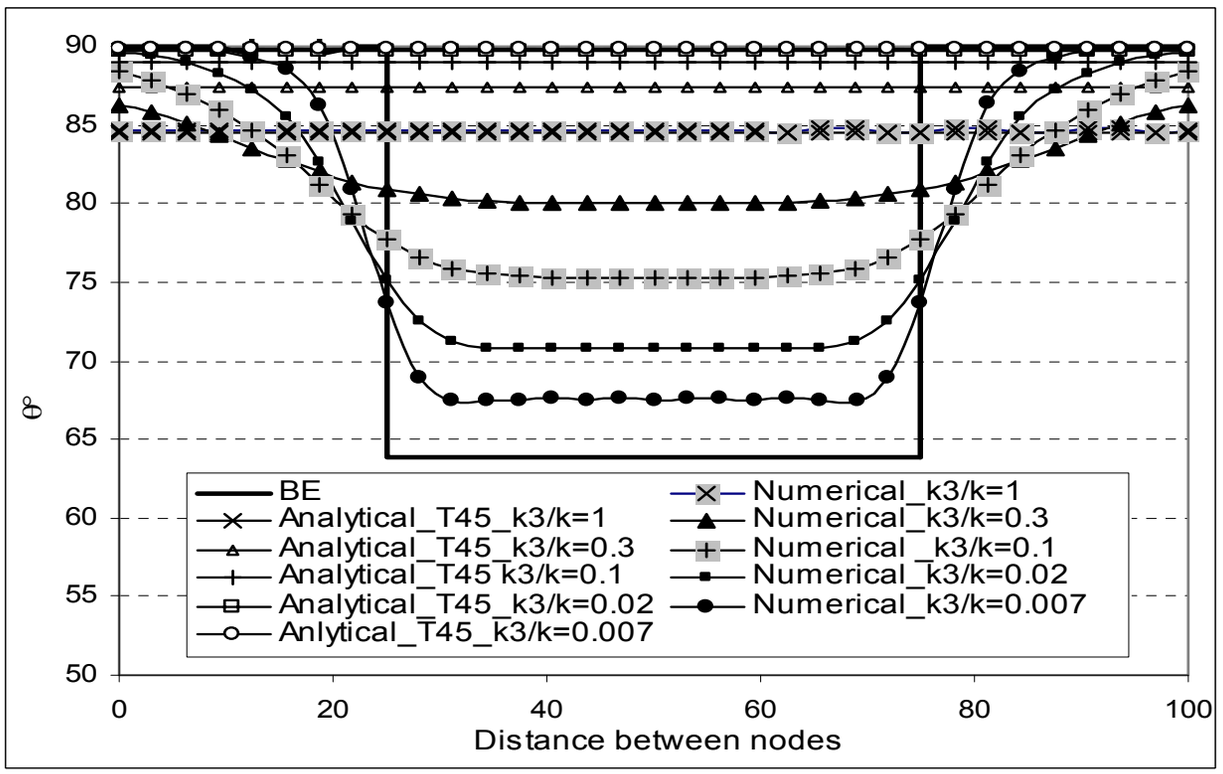

Figure 12. Comparison between Numerical and Predicted angles between yarns along the path 1 in FEM1.

Figure 12 demonstrated that the value of the angle between yarns was not uniform in the central zone of the FEM and it was not null in ends of the path1. For three FEM, the numerical angle between yarns tend to verify the predict angle (solid line) in the Bias Extension test for the lower value of $\frac{k_3}{k}$ This is another reason to justify the influence of the ration of rigidities on the shearing deformation of woven.

3.4. Elongation of yarns

Under the pin-joint assumption for trellising deformation mode, the edge length of the membrane element should remain unchanged during the deformation; thus the Green Lagrange stretch Eg_{11} and Eg_{22} should be null in Bias Extension test:

$$E_{g11} = E_{g22} = 0 \tag{41}$$

In Tensile test on 45°, warp and weft yarns are submitted respectively to Green Lagrange deformations $E_{g_{11}}$ and $E_{g_{22}}$ as follows:

$$E_{g_{11}} = \frac{1}{2}(\left|\boldsymbol{F}.\vec{g}_1\right|^2 - 1) = \frac{k_1 - k_{12}}{2(k_1 k_2 - k_{12}^2)}\frac{E_{11}}{C_{45}} \tag{42}$$

$$E_{g_{22}} = \frac{1}{2}(\left|\boldsymbol{F}.\vec{g}_2\right|^2 - 1) = \frac{k_2 - k_{12}}{2(k_1 k_2 - k_{12}^2)}\frac{E_{11}}{C_{45}} \tag{43}$$

In the case of balanced fabric without coupling between elongations in yarns directions, the warp and weft yarns are submitted to the same elongation:

So

$$E_{g11} = E_{g22} = E \tag{44}$$

Where

$$E = \frac{k_3}{k + k_3}E_{11} \tag{45}$$

In Figure 13, we compared numerical stretch deformation along the second path and the predicted elongation in yarn direction.

In the first hand, we noticed that the numerical elongation was not null. It became more important by increasing the value of $\frac{k_3}{k}$ in all FEM. In another hand, numerical value of elongation is closely conforming to the expected value in the tensile test in 45° for different values of $\frac{k_3}{k}$ in all FEM. This analysis provided that during Bias Extension test, yarns are

subjected a few elongation. These stretches depend of the value of the ratio between shearing and tensile rigidities of woven. Same previous analyses are taken also along the third vertical path (Path3) and same results are verified.

Figure13 represented the evolution of $\frac{S_2}{S_1}$ versus $\frac{E_2}{E_1}$ along the third path. Like the first path, for few values of $\frac{k_3}{k}$, the shearing is the utmost deformation. But in all cases, the Bias Extension test is characterized by the tensile state.

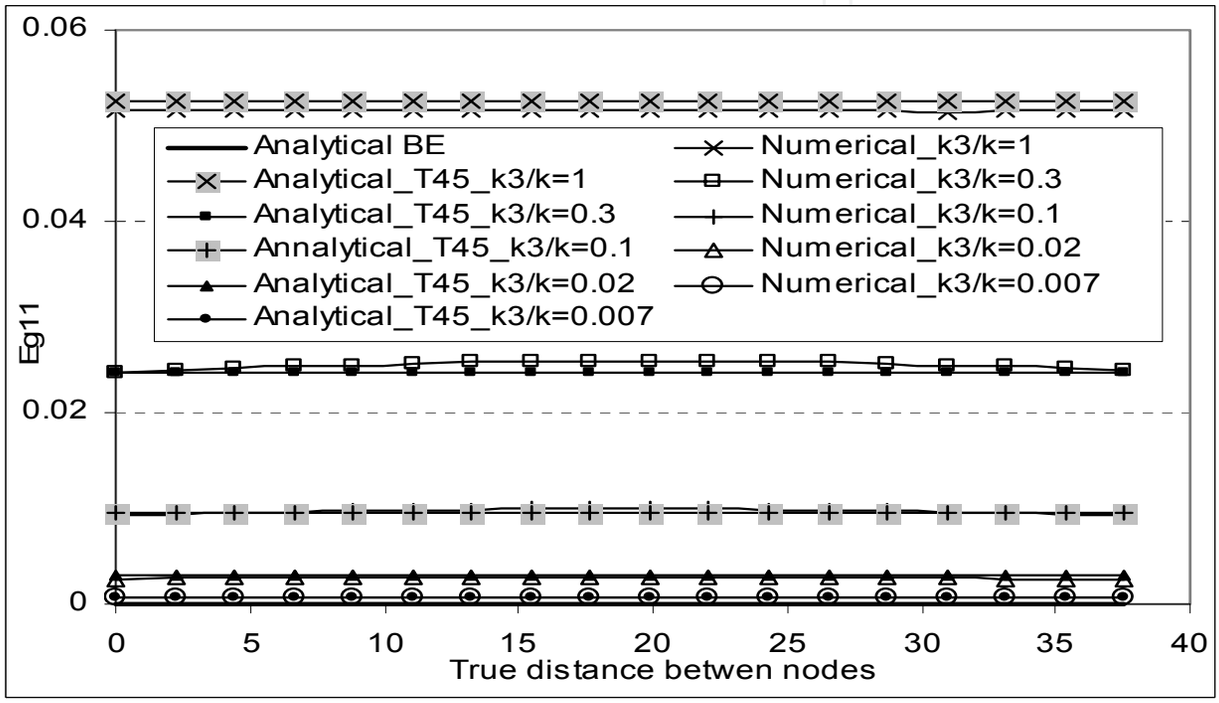

Figure 13. Variation of E_{g11} along the path 2in FEM1.

4. Conclusion

In this work, an orthotropic hyperelastic model test of woven fabric is developed and implanted into Abaqus/explicit to simulate Bias-Extension at low displacement. The analysis of numerical answers along longitudinal and transversal middle paths, proved, in the first hand, that to decreasing the ratio between shearing and tensile rigidities, the state deformation became to be conform to that predicted by the proposed model in the Bias Extension test for all FEM. In another hand, the angle between yarns tends to verify the predicted angle during the Bias Extension test. Although the stress state, is conform to the expected analysis of Traction test on 45°. The analysis of Green Lagrange stretching strain in the yarns direction, demonstrated that there was an elongation of yarns during test for different shearing rigidity. This elongation was exactly conforming to the predicted analytical elongation in the Traction test in 45°. Curves of Force versus displacement of the

Traction test in 45° applied to of the central zone A is closely to the numerical answers. We are able to adjust both curves by coefficients of adjustment.

This study allowed to verify analytical hypothesis adopted to interpret the Bias Extension test. The comparison between in Bias Extension test, the shearing deformation depends of the ratio between shearing and tensile rigidities of fabric. In Spite of the low displacement, this test presented always a stress state.

Author details

Samia Dridi
Department of Mechanics of Structures and Materials of the ISAE,
Institute Superieur of the Aeronautique and the Space, Edouard Belin, Toulouse, France

5. References

[1] Naujokaitytė L, Strazdienė E, Domskienė J (2008) Investigation of Fabric Behaviour in Bias Extension at Low Loads. Fibres & Textiles 16:59-63
[2] Zheng J, Komatsu T, Yazaki Y, Takater M, Inui S, Shimizu Y. (2006) Evaluating Shear Rigidity of Woven Fabrics. Textile Research Journal 76:145-151.
[3] Alamdar-Yazdi A (2004) A New Method to Evaluate Low-stress Shearing Behavior of Woven Fabrics. Fibres& Textiles 29:333-338.
[4] Dobb B, Russell S (1995). A System for the Quantitative Comparison of Wrinkling in Plain Fabrics. The Journal of the Textile Institute 86:495-497.
[5] Domskienė J, Strazdienė E (2005) Investigation of Fabric Shear Behavior. Fibres & Textiles 13:26-30.
[6] Mahar T.J, Ajiki I, Dhingra R.C, Postle R(1989) Fabric Mechanical and Physical Properties Relevant to Clothing Manufacture. International journal of clothing science and technologies 1:6-13.
[7] Lebrun G, Bureau M.N, Denault J (2003) Evaluation of bias-extension and picture-frame test methods for the measurement of intraply shear properties of PP/glass commingled fabrics. Composite Structures 61:341–352.
[8] Sharma S.B, Sutcliffe M.P.F, Chang S.H (2003) Characterisation of Material Properties for Draping of Dry Woven Composite Material. Composites Part A 34:1167–1175.
[9] Harrison P, Clifford M.J, Long A.C (2004).Shear Characterisation of Viscous Woven Textile Composites: a comparison between picture frame and bias extension experiments. Composites science and technology 64:1453–65.
[10] Potluri P, Perez Ciurezu D.A, Ramgulam R.B (2006) Measurement of Meso-scale Shear Deformations for Modelling Textile Composites. Composite Part A 37:303–314.
[11] Lomov S.V, Verpoest I (2006) Model of Shear of Woven Fabric and Parametric Description of Shear Resistance of Glass Woven Reinforcements. Composites Science and Technology 66: 919–933.

[12] Launay J, Hivet G, Duong A.V, Boisse P.(2008) Experimental Analysis of the Influence of Tensions on in Plane Shear Behaviour of Woven Composite Reinforcements. Composites Science and Technology 68:506–515.
[13] Kilby W.F (1963) Planar Stress-Strain Relationships in Woven Fabrics. The Journal of the Textile institute 54:9-27.
[14] Yick K.L, Chen K.P.S, Dhingra R.C, How Y.L(1966) Comparison of Mechanical Properties of Shirting Materials Measured on the KES-F and FAST Instruments. Textile Research Journal 66:622-633.
[15] Yu WR, Pourboghrat F, Chung K, Zampaloni M, Kang TJ (2002) Non Orthogonal Constitutive Equation for Woven Fabric Reinforced Thermoplastic Composites. Composite Part A 33:1095–1105.
[16] Yu X, Cartwright B, McGuckin D, Ye L, Mai Y.W (2006) Intra-ply Shear Locking In Finite Element Analyses of Woven Fabric Forming Process. Composites Part A 37:790-803.
[17] Sidhu R.M, Averill R.C, Riaz M, Pourboghrat F (2001) Finite Element Analysis of Textile Composite Perform Stamping. Composite Structures 52:483-497.
[18] Aimène Y, Vidal-Sallé E, Hagège B, Sidoroff F, Boisse P (2010) A Hyperelastic Approach for Composite Reinforcement Large Deformation Analysis. Journal of Composite Materials 44:5-26.
[19] Guo Z.Y, Peng X.Q, Moran B (2006) A Composite-based Hyperelastic Constitutive Model for Soft Tissue with Application to the Human Annulus Fibrosus. Journal of the Mechanics and Physics of Solids 54:1952-1971.
[20] Diani J, Brieu M, Vacherand J, Rezgui A (2004) Directional Model for Isotropic and Anisotropic Hyperelastic Rubber-like Materials. Mechanic of Materials 36:313-321.
[21] Bonet J, Wood R.D (1997) Non Linear Continuum Mechanics for Finite Element Analysis. Cambridge University Press.
[22] Zouari R, Amar S.B Dogui,A (2008) Experimental and Numerical Analyses of Fabric off-axes Tensile Test. The Journal of the Textile Institute 35:1-11.
[23] Dogui A (1988) Cinématique Bidimensionnelle en Grandes Déformations : Application à la traction hors axes et à la torsion. Journal de Mécanique Théorique et Appliqué 7:43-64.
[24] Mark C,Taylor H. M(1956) The fitting of Woven Cloth to Surfaces. The Journal of the Textile Institute 47:47-48.
[25] Lindberg J, Behre B, Dahlberg B (1961) Shearing and Buckling of Various Commercial Fabrics. Textile Research Journal 36:99-122;
[26] Skelton J (1976) Fundamentals of fabric shear. Textile Research Journal 46:862-869.
[27] Potter K(1979) The influence of Accurate Stretch Data for Reinforcements on the Production of Complex Structural Mouldings. Composites 10:161-173.
[28] Potter K (2002) Bias Extension Measurement on Cross Plied Unidirectionnel Prepreg. Composites Part A 33:63-67.
[29] Xiaobo Y, Bruce C, Damian M, Lin Y, Yiu W (2006) Intra-ply Shear Locking in Finite Element Analyses of Woven Fabric Forming Processes, Composites Part A 37:790–803.

[30] Tenthijie R.H.W, Akkeman R (2008) Solution to Inter Ply Shear Locking in Finite Element Analyses of Fibre Reinforced Material. Composite Part A 39:1167-1176.

IntechOpen